

Topological interface states – a possible path towards a Landau-level laser in the THz regime

Mark O. Goerbig^{1,*}

¹*Laboratoire de Physique des Solides, Université Paris Saclay,
CNRS UMR 8502, F-91405 Orsay Cedex, France*

(Dated: July 12, 2023)

Volkov-Pankratov surface bands arise in smooth topological interfaces, *i.e.* interfaces between a topological and a trivial insulator, in addition to the chiral surface state imposed by the bulk-surface correspondence of topological materials. These two-dimensional bands become Landau-quantized if a magnetic field is applied perpendicular to the interface. I show that the energy scales, which are typically in the 10 – 100 meV range, can be controlled both by the perpendicular magnetic field and the interface width. The latter can still be varied with the help of a magnetic-field component in the interface. The Landau levels of the different Volkov-Pankratov bands are optically coupled, and their arrangement may allow one to obtain population inversion by resonant optical pumping. This could serve as the elementary brick of a multi-level laser based on Landau levels. Moreover, the photons are absorbed and emitted either parallel or perpendicular to the magnetic field, respectively in the Voigt and Faraday geometry, depending on the Volkov-Pankratov bands and Landau levels involved in the optical transitions.

I. INTRODUCTION

Landau levels (LLs), which arise due to the quantization of the electrons' energy in a strong magnetic field, have been regularly proposed to be a promising system for a frequency-tunable laser in the THz regime [1–5]. Indeed, upon a putative population inversion between the LLs n and $n + 1$ in parabolic bands, one may expect cyclotron emission with a typical frequency $\Omega_{n+1,n} = \omega_c$ given by the cyclotron frequency $\omega_c = eB/m_B$, which is directly controlled by the strength of the magnetic field B and the band mass m_B . In spite of this conceptually appealing proposal, the path to the realization of a working LL laser is barred by strong obstacles that are mainly concerned with population inversion. The latter requires rather long-lived electrons in the excited LL, but their lifetime is strongly reduced by non-radiative recombinations, namely Auger processes that are prominent due to the equidistant LL separation [6] (for a detailed discussion of these processes, see Ref. [7]). In such processes, an electron in the excited LL $n + 1$ can be promoted due to electron-electron interactions to the LL $n + 2$ while the required energy is provided by a simultaneous desexcitation of another electron from $n + 1$ to n . Instead of using one excited electron to emit a photon of frequency ω_c , two electrons in the LL $n + 1$ are thus lost without emission of any photon. Another obstacle equally related to equidistant LLs is reabsorption of cyclotron light due to the transition $(n + 1) \rightarrow (n + 2)$, which is resonant with the $(n + 1) \rightarrow n$ transition used in the emission of light [7–9].

Soon after the isolation of graphene, physicists explored this material in cyclotron-emission experiments in the perspective of realizing a LL laser [4, 5, 10].

Due to the linearly dispersing bands of graphene electrons in the vicinity of charge neutrality, the LL spectrum is given by $E_n = \pm \hbar(v/l_B)\sqrt{2n}$, in terms of the Fermi velocity $v \simeq 10^6$ m/s and the magnetic length $l_B = \sqrt{\hbar/eB} \simeq 26$ nm/ $\sqrt{B[\text{T}]}$, *i.e.* the levels are no longer equidistant. While the orders of magnitude with a fundamental gap of $\hbar\Omega_{1,0} \sim 100$ meV for magnetic fields $B \sim 10$ T are promising for possible THz applications, Auger processes remain a relevant source of non-radiative recombination processes also in these relativistic systems [11]. For example, while the $1 \rightarrow 0$ transition is no longer in resonance with the neighboring $2 \rightarrow 1$ transition, it is in resonance with the transition $4 \rightarrow 1$ due to the square-root dependence of the LL levels on the level index n [7, 12]. Furthermore, it has been shown that the optical phonon responsible for the G band in graphene (at ~ 200 meV) also enhances decay processes that are detrimental to population inversion [13]. The drawback of resonant transitions and enhanced Auger processes can to some extent be healed, *e.g.* in gapless HgTe/CdTe quantum wells, where the low-energy electrons are described in terms of so-called Kane fermions. While their zero-field spectrum is similar to that of massless Dirac fermions, LLs with even indices are absent in the spectrum so that some transitions are absent, such as the above-mentioned transition $4 \rightarrow 1$.

An extremely interesting route towards the realization of a LL laser is the use of Dirac materials with a (mass) gap Δ that is on the same order of magnitude as the typical LL spacing, *i.e.* in the 100 meV range, for systems with a characteristic velocity parameter of $v \simeq 10^6$ m/s. In this case, the LL spectrum is given by

$$E_{\lambda,n} = \lambda \sqrt{\Delta^2 + 2\hbar^2 v^2 n / l_B^2}, \quad (1)$$

where $\lambda = \pm$ is the band index. Indeed, if $\Delta \sim \hbar v / l_B$, the LL spectrum is neither (approximately) linear in n and B as it would be in the limit $\Delta \gg \hbar v / l_B$ nor does

* mark-oliver.goerbig@universite-paris-saclay.fr

it follow the square-root dependence of graphene in the opposite limit $\Delta \ll \hbar v/l_B$. In this case, the absence of simultaneous resonant transitions suppress both reabsorption and non-radiative Auger scattering. First encouraging results in this direction have been obtained in gapped HgTe/CdTe quantum wells [9]. Another system in which massive Dirac fermions occur is the interface of a topological and a trivial insulator, in the form of Volkov-Pankratov (VP) states [14–16]. The bulk-surface correspondence for topological materials enforces indeed the occurrence of a massless chiral state at such an interface, but it has been shown that the interface spectrum is much richer in systems with smooth interfaces, *e.g.* when the gap changes over a certain distance ℓ that characterizes the interface width and that is larger than an intrinsic length $\lambda_C = \hbar v/\Delta$. In smooth interfaces between a topological and a trivial insulator, one finds a whole family of surface states the spectrum of which is indeed given by [16]

$$\epsilon_m(\mathbf{q}) \simeq \lambda \hbar v \sqrt{\mathbf{q}^2 + 2m/l_S^2}. \quad (2)$$

Here, $\mathbf{q} = (q_x, q_y)$ is the two-dimensional (2D) wave vector in the interface, m denotes the index of the surface band, and $l_S = \sqrt{\ell \lambda_C}$ is a characteristic length determining the extension of the interface states in the z direction perpendicular to the interface. Equation (2) is indeed valid as long as the energy of the surface bands at $\mathbf{q} = 0$ is smaller than the bulk gap, $\sqrt{2m\hbar v}/l_S \leq \Delta$. The latter condition is equivalent to requiring that the interface width ℓ be larger than m times the intrinsic length λ_C [16]. The $n = 0$ surface state is precisely the chiral state that survives in the abrupt limit, $\ell \rightarrow 0$, while the VP states (for $m \neq 0$) disappear in the continuum of bulk states as soon as $\ell < \lambda_C$. Notice that the formation of VP states is a universal property of topological materials that has been studied not only in topological insulators [16–20], but also in Weyl semimetals [21, 22], graphene [23], and topological superconductors [24].

Very recently, inter-VP transitions have been measured within magneto-optical spectroscopy in $\text{Pb}_{1-x}\text{Sn}_x\text{Se}$ crystals [25] in which the Sn concentration determines whether the system is a trivial or a topological (crystalline) insulator [26–28]. Moreover, the concentration determines the size of the bulk gap so that smooth interfaces may be obtained by molecular-beam epitaxy (MBE) in which the Sn concentration is smoothly varied during the growth process, and where the absolute band gap in the topological regime can be designed such as to be identical to that in the trivial insulator [25]. This allows for a strong versatility in the fabrication of interfaces of various widths and thus of systems with specially designed fundamental gaps

$$\Delta_{\text{VP}} = \sqrt{2}\hbar v/l_S = \sqrt{2}\Delta \sqrt{\frac{\lambda_C}{\ell}} = \sqrt{\frac{2\hbar v\Delta}{\ell}} \quad (3)$$

between the $m = 1$ VP and the chiral ($m = 0$) surface states.

In the present paper, I argue that smooth topological interfaces, such as in the above-mentioned $\text{Pb}_{1-x}\text{Sn}_x\text{Se}$ crystals, may be extremely promising systems for the realization of long-lived population inversion if a magnetic field is applied perpendicular to the interface that quantizes the 2D electronic motion in the interface into LLs. The main reason for this expectation is the fact that VP bands provide us with several families of LLs that can to some extent be brought into close energetic proximity with LLs of the chiral surface band. This would allow for devices similar to three- or four-level lasers in which population inversion could be more easily achieved than in the usual LL setup. Furthermore, optical pumping and radiative desexcitation can be chosen to happen in different directions via an intelligent choice of the involved transitions. Indeed, while the optical selection rules in the Faraday geometry impose that the emitted or absorbed photons propagate in the direction of the magnetic field for a transition coupling the LLs n and $n \pm 1$, it has been shown previously [29] that such transitions must obey an optical selection rule $m \rightarrow m$ for the VP states. The selection rules are inverted in the Voigt geometry, where the emitted or absorbed photon propagates in a direction perpendicular to the magnetic field. The underlying reason for these selection rules and their geometry dependence is an intriguing analogy between the spatially changing gap parameter and LL quantization. Indeed, the spatially varying gap parameter can be viewed as a fake magnetic field that is oriented in the plane of the interface, and the characteristic length l_S plays the role of an effective magnetic length. Via an intelligent choice of the geometry of a cavity hosting the topological material and the involved transitions, one may therefore expect to obtain a strong cyclotron emission in the direction of the interface while pumping the system with photons propagating perpendicular to the interface, or *vice versa*.

II. VOLKOV-PANKRATOV STATES AND OPTICAL SELECTIONS IN A MAGNETIC FIELD

Let us first review some basic features of VP states and their coupling to light in the presence of a magnetic field along the lines of Ref. [29]. We consider an interface between a trivial insulator in the lower part of the device ($z < -\ell$) and a topological one in the upper part ($z > \ell$) (see inset of Fig. 1). Due to the magnetic field, the VP bands (2) get quantized into LLs whose spectrum reads (for $n \neq 0$)

$$E_{\lambda, m, n \neq 0} = \lambda \hbar v \sqrt{\frac{2|m|}{l_S^2} + \frac{2|n|}{l_B^2}}, \quad (4)$$

where we have considered the magnetic field to be oriented perpendicular to the interface (in the z -direction). For notational simplicity, we merge the band index λ from now on with the VP and LL indices so that

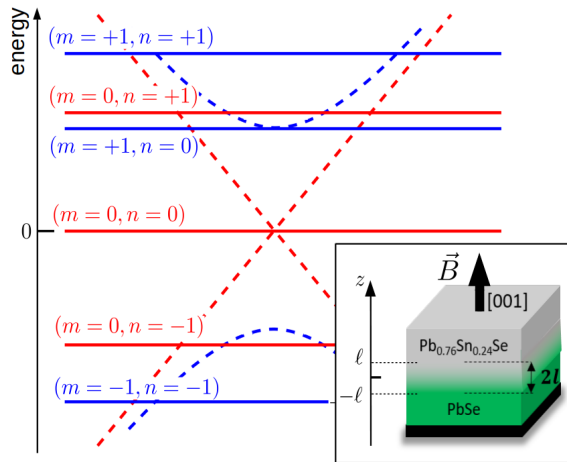


FIG. 1. Landau levels for VP surface states. The red levels correspond to the chiral surface state with $m = 0$, while the blue levels correspond to the $m = \pm 1$ VP states. The sign indicates the band index λ here for notational convenience. As a consequence of the parity anomaly, the $n = 0$ LL is found only in the upper VP band ($m = +1$). The inset, adapted from Ref. [25], shows the setup of a smooth interface between a trivial insulator (PbSe) at $z < -\ell$ and a topological insulator ($\text{Pb}_{0.76}\text{Sn}_{0.24}\text{Se}$) at $z > \ell$. The magnetic field is oriented in the $[001]$ direction perpendicular to the interface.

$(-m, -n)$ corresponds to the n -th LL in the m -th VP band of negative energy ($\lambda = -$), whence the modulus of the indices in the spectrum (4) to avoid confusion. Due to the parity anomaly, the above spectrum is only valid for LLs with an index $n \neq 0$, while the $n = 0$ LLs of the VP bands stick either to the bottom of the positive-energy bands ($\xi = +$) or to the top of the negative-energy VP state ($\xi = -$)

$$E_{m,n=0} = \xi \hbar v \sqrt{\frac{2|m|}{l_S^2}}, \quad (5)$$

depending on the chirality index ξ . The latter can be changed if we change the order between the topological and the trivial insulator (interface between a topological insulator in the lower part and a trivial one in the upper part), and it can also be altered easily by changing the orientation of the magnetic field. The LL spectrum for the $m = 0$ and the $m = 1$ VP states [both for the conduction ($m = +1$) and the valence band ($m = -1$)] are shown in Fig. 1. Notice that the surface-state-width parameter l_S can be decreased effectively with the help of an *inplane* magnetic field B_{\parallel} , $l_S(B_{\parallel} = 0)^{-4} = 1/\ell^2 \lambda_C^2 \rightarrow l_S^{-4} = l_S(B_{\parallel} = 0)^{-4} + (eB_{\parallel}/\hbar)^2$ so that the effective energy separation between the VP states, given by Eq. (3) is increased to [29]

$$\Delta_{\text{VP}} = \sqrt{\frac{2\hbar v \Delta}{\ell}} \left(1 + \frac{e^2 v^2 B_{\parallel}^2 \ell^2}{\Delta^2} \right)^{1/4}. \quad (6)$$

geometry	VP states	Landau levels
Faraday	$m \rightarrow \pm m$	$\pm n \rightarrow n \pm 1$
Voigt	$m \rightarrow \pm m \pm 1$	$n \rightarrow \pm n$

TABLE I. Optical selection rules in the Faraday (photon propagation perpendicular to the interface) and the Voigt geometry (photon propagation in the interface).

The writing of Eq. (4) unveils the reminiscence of LLs and VP states. Indeed, if we linearize the gap inversion over the smooth interface by a linear function connecting a gap parameter of $+\Delta$ in the trivial insulator (at $z < -\ell$) and $-\Delta$ in the topological insulator (at $z > \ell$), *i.e.* $-\Delta z/\ell$, the system may be mapped to the LL problem of massive Dirac fermions [16]. Within this analogy, the variation of the gap parameter in the z -direction may be viewed as a vector potential that stems from a “fake” magnetic field oriented in the interface, while the physical magnetic field is oriented in the z -direction. Notice furthermore that the above description can easily be generalized to a situation where the gap in the topological insulator is not of the same size as that in the trivial one [16], in which case the effective interface width l_S is determined by an average between the two gaps. The analogy between interface width and magnetic field finally yields a physical understanding of the optical selection rules between the levels (m, n) and (m', n') , where henceforth the first index indicates the VP band and the second one the physical LL. In the Faraday geometry, in which the absorbed or emitted photon propagates in the direction of the magnetic field, angular-momentum conservation imposes that the only optically active transitions involve adjacent LL indices, $n \rightarrow n' = \pm(n \pm 1)$, regardless of the band index λ . This needs to be contrasted to the Voigt geometry, where the photon propagates in the plane perpendicular to the magnetic field and where the LL index remains unchanged $n \rightarrow n' = \pm n$. Since the fake magnetic field that yields the VP bands is oriented in the interface, Voigt and Faraday geometry are inverted, and a photon propagating perpendicular to the interface couples VP bands with the same index ($m \rightarrow m' = \pm m$) while a photon with a wave vector in the interface couples adjacent VP bands [$m \rightarrow m' = \pm(m \pm 1)$]. As in the LL problem, the selection rules, which are summarized in the table above, do not depend on the band index. In both cases, VP states and LLs, it is the circular polarization of the photon determines which of the adjacent levels or bands are optically coupled.

III. THREE-LEVEL SCHEME

Let us first illustrate schematically the different emission processes in terms of resonant (optical) pumping within a three-level picture to fix some basic ideas. In a first step, we consider the situation depicted in Fig. 2(a) where the LL energy scale $\sqrt{2\hbar v}/l_B$ is slightly larger than the VP gap Δ_{VP} given in Eq. (3), *i.e.* the mag-

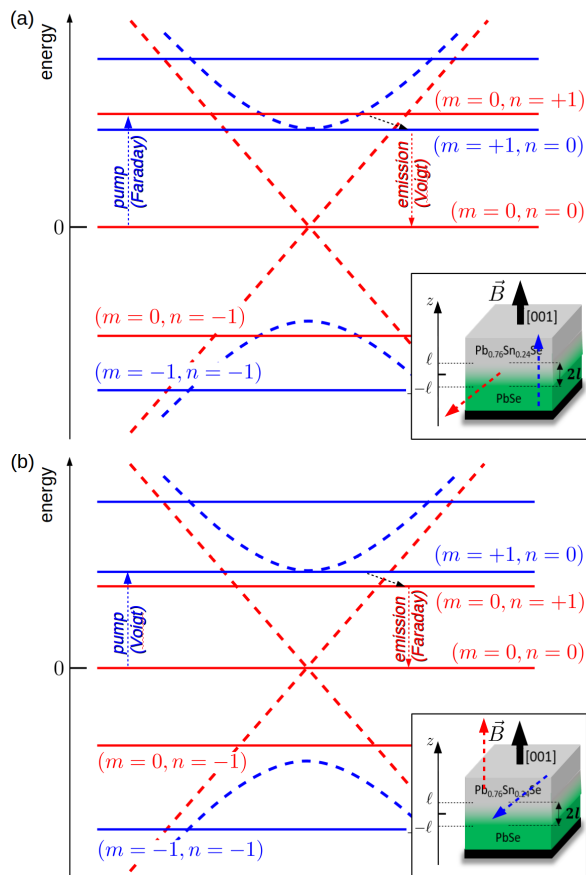


FIG. 2. Sketch of a three-level scheme for stimulated cyclotron emission. Ideally, the Fermi level is considered to be situated above the $(m = 0, n = 0)$ level so that the zero-energy level is filled. (a) Pumping in the Faraday geometry for $\sqrt{2}\hbar v/l_B > \Delta_{VP}$. The $(m = 0, n = 1)$ level is populated via pumping (dashed blue arrow) from the zero-energy $(m = 0, n = 0)$ level, and emission can take place in the Voigt geometry in the transition $(m = 1, n = 0) \rightarrow (m = 0, n = 0)$ (dashed red arrow). The level $(m = 1, n = 0)$ is rapidly populated by the $(n = 1, m = 0)$ level if the latter is almost resonant with the former, via a rapid non-radiative decay (dashed black arrow). (b) Similar process with pumping in the Voigt geometry for $\sqrt{2}\hbar v/l_B < \Delta_{VP}$. The pumping transition is $(m = 0, n = 0) \rightarrow (m = 1, n = 0)$ (dashed blue arrow) while emission takes place in the $(m = 0, n = 1)$ transition (dashed red arrow) that is populated via rapid non-radiative decay processes (dashed black arrow) from the $(m = 1, n = 0)$ level, which is slightly higher in energy. The insets represent the device geometries, with the direction of propagation of the absorbed (dashed blue arrow) and emitted (dashed red arrow) photon, for the two configurations, respectively.

netic length is slightly smaller than the effective surface width l_S . We show below in Sec. V that this situation can be easily achieved *e.g.* in MBE-grown $\text{Pb}_{1-x}\text{Sn}_x\text{Se}$ crystals. In this case, the $n = 1$ LL of the chiral $m = 0$ surface state is slightly above the $n = 0$ level of the upper VP band with an index $m = 1$. In Fig. 2(a), we consider optical pumping in the Faraday ge-

ometry, where the light frequency is resonant with the $(m = 0, n = 0) \rightarrow (m = 0, n = 1)$ transition. If the target level is only slightly above the lowest LL of the $m = 1$ VP band, $(m = 1, n = 0)$, one may expect rapid non-radiative decay of the excited electrons to the latter level. These electrons may then decay to the zero-energy level $(m = 0, n = 0)$ by emitting light of the frequency $\omega = \sqrt{2}v/l_S$ in the Voigt geometry, *i.e.* absorbed and emitted photons, even if they may be almost resonant, propagate in perpendicular directions. While the magnetic field does then not allow one to control the frequency of the transition, which is determined by the interface width ℓ , it allows us to bring the levels $(m = 1, n = 0)$ and $(m = 0, n = 1)$ into close energetic vicinity and thus to increase the transition rate between the two levels, which is proportional to [30]

$$\Gamma \sim \frac{1/\tau}{1/\tau^2 + 2v^2(1/l_B - 1/l_S)^2}, \quad (7)$$

if we consider Lorentzian level broadening due to a dephasing time τ []. For a typical value of $\tau \sim 100$ fs, the level broadening is then on the order of some meV. Notice, however, that the frequency of the emitted light may to some extent be varied with the help of an inplane magnetic field, according to Eq. (6).

Similarly, one may use the Voigt geometry for pumping the transition $(m = 0, n = 0) \rightarrow (m = 1, n = 0)$. If the latter is now slightly above the $(m = 0, n = 1)$ level [see Fig. 2(b)], *i.e.* for smaller magnetic fields with $\sqrt{2}\hbar v/l_B < \Delta_{VP}$, the $n = 1$ LL of the chiral surface band may be populated by non-radiative decay processes, and one may expect a population inversion between the $(m = 0, n = 0)$ and $(m = 0, n = 1)$ levels, with cyclotron emission at the fundamental frequency $\omega_C = \sqrt{2}v/l_B$. As before, the emitted photon propagates then in a direction perpendicular to that of the absorbed photon, but Faraday and Voigt geometries are inverted.

IV. FOUR-LEVEL SCHEME

We now investigate a possible four-level scheme for population inversion, as shown in Fig. 3. For the sake of the argument, we consider the $n = 0$ LLs of the VP bands now to be situated in the negative-energy branch. As already mentioned, this can easily be achieved by switching the orientation of the magnetic field. Let us choose optical pumping by light in the Voigt geometry that is resonant with the transition $(m = 0, n = -1) \rightarrow (m = 1, n = 1)$. In contrast to the three-level scheme discussed in the previous section, the target level is no longer in close vicinity with the level below that is $(m = 0, n = 1)$. However, both are optically coupled, and an electron can transit from $(m = 1, n = 1)$ to $(m = 0, n = 1)$ by emitting a photon in the Voigt geometry again. While this photon is sacrificed in the present scheme, its emission allows for an enhanced population of the $n = 1$ LL in

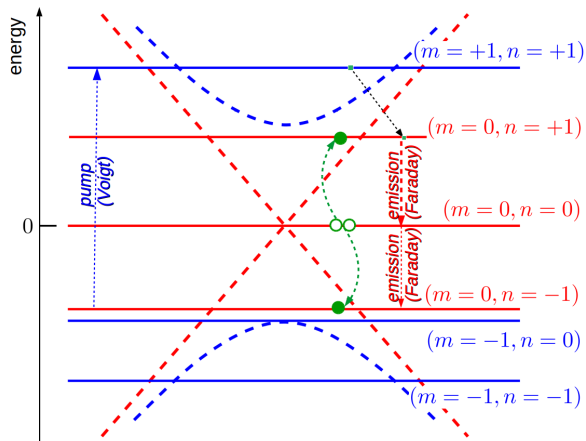


FIG. 3. Sketch of a four-level scheme for stimulated cyclotron emission. Ideally, the Fermi level is now situated below the $(m = 0, n = 0)$ level so that the zero-energy level is empty. We consider pumping in the Voigt geometry for $\sqrt{2}\hbar v/l_B < \Delta_{VP}$ and a situation, where the $n = 0$ LL of the $m = 1$ VP state is in the negative-energy branch. The $(m = 1, n = 1)$ level is populated via pumping (dashed blue arrow) from the $(m = 0, n = -1)$ level, and the pumped electrons can decay radiatively to the $(m = 0, n = 1)$ level by emitting light also in the Voigt geometry. Electrons in the $(m = 0, n = 1)$ LL can then decay to the zero-energy level $(m = 0, n = 0)$ emitting cyclotron light in the direction perpendicular to the interface (in the Faraday geometry, dashed red arrows). Furthermore, this transition is resonant with that $(m = 0, n = 0) \rightarrow (m = 0, n = -1)$, and a second photon with the cyclotron frequency can thus be emitted. Auger processes, shown in green now enhance the depopulation of the zero-energy LL $(m = 0, n = 0)$ and are therefore helpful for cyclotron emission.

the chiral surface band. This is particularly interesting since the transition $(m = 0, n = 1) \rightarrow (m = 0, n = 0)$ to the central zero-energy level, which we consider to be non or only sparsely populated, is resonant with the $(m = 0, n = 0) \rightarrow (m = 0, n = -1)$ transition to the original level served in the pumping process. Under strong pumping and thus a strong depletion of the $(m = 0, n = -1)$ level, it is therefore possible to emit *two* photons at the cyclotron frequency.

It is noteworthy that the above-mentioned resonant cyclotron transitions are also involved in non-radiative Auger processes. Such Auger processes have been shown to be detrimental to population inversion in GaAs and graphene. Here, however, this is not the case. Indeed, one of the two electrons that take part in the Auger process, where both electrons originally reside in the $(m = 0, n = 0)$ LL, is kicked back into the $(m = 0, n = 1)$ LL thus maintaining the fertile population inversion. While the electron that transits simultaneously to the level $(m = 0, n = -1)$ is energetically lost, *i.e.* it does not emit a photon, the first electron emits another photon at the cyclotron frequency before it can take part in another Auger process or radiatively transit to $(m = 0, n = -1)$.

V. POSSIBLE REALIZATION IN $\text{Pb}_{1-x}\text{Sn}_x\text{Se}$ CRYSTALS

While the above arguments are not restricted to a particular topological insulator, it is useful to discuss the orders of magnitude of the probably best controlled system in which VP states occur that is MBE-grown $\text{Pb}_{1-x}\text{Sn}_x\text{Se}$ crystals [26–28]. As mentioned in the introduction, the MBE growth allows one to obtain interfaces with a well-controlled interface width in which the VP states obey to great accuracy the dispersion (2) [25]. Most saliently, the Sn concentration x in the Pb substitution allows one to trigger the electronic nature of the material. While, for $x = 0$, the system is a trivial band insulator it becomes a crystalline topological insulator above a critical concentration on the order of ($x_c \simeq 0.12$). Moreover, the Sn concentration determines the size of the gap, which is on the order of 90 meV in the trivial insulator at $x = 0$ [27, 28]. The choice $x = 0.24$ allows one to obtain the same magnitude for the gap in the topological insulator ($2\Delta \sim 90$ meV) [25], but even larger gaps on the order of $2\Delta \sim 200$ meV may be obtained upon variation of temperature and strain on the crystals [26, 28]. Magneto-optical experiments indicate that the fundamental VP gap (3) scales as [25]

$$\Delta_{VP} \simeq 45 \text{ meV} / \sqrt{\ell/100 \text{ nm}}, \quad (8)$$

and samples with interface widths between $\ell = 50$ and 200 nm have been obtained, while the intrinsic length has been estimated to be $\lambda_C \simeq 6$ nm so that the effective surface width varies between $l_S \sim 17$ nm and $l_S \sim 35$ nm. In order for the magnetic length to be on the same order of magnitude as l_S – situation considered in the present paper – one would require magnetic fields in the range 0.5...3 T that are easily accessible experimentally.

Finally, the Fermi velocity is roughly half of that in graphene so that $v/c \sim 1/600$, in terms of the speed of light c . If we consider the fundamental cyclotron resonance associated with the transition $(m = 0, n = 1) \rightarrow (m = 0, n = 0)$, the energy of the transition is thus roughly

$$\sqrt{2} \frac{\hbar v}{l_B} \simeq 20 \text{ meV} \times \sqrt{B[\text{T}]}. \quad (9)$$

This implies a the transition rate [4]

$$\begin{aligned} \Gamma_{(m=0,n=1) \rightarrow (m=0,n=0)} &= 2\alpha \left(\frac{v}{c}\right)^2 \omega \\ &\simeq 2.4 \times 10^6 \text{ s}^{-1} \times \sqrt{B[\text{T}]}, \end{aligned} \quad (10)$$

in terms of the fine-structure constant $\alpha = 1/137$, if we consider dipolar light coupling. This is roughly a factor of four smaller than in graphene due to the reduced Fermi velocity v . Notice that interaction-induced decay processes take place at much shorter time scales, typically in the fs range. In the case of almost resonant levels, as discussed in the previous section [see *e.g.* the levels

($m = 1, n = 0$) and ($m = 0, n = 1$) in Fig. 2(a) and (b)], the decay rate from the higher to the lower level is on the order of [30]

$$\Gamma \sim \frac{2\pi}{\hbar} \left(\frac{e^2}{\epsilon l_B} \right)^2 \left(\frac{\tau}{\hbar} \right) \simeq \epsilon^{-1} \times 10^{16} \text{ s}^{-1} \times B[\text{T}], \quad (11)$$

where ϵ is the dielectric constant of the host material.

VI. CONCLUSIONS

In conclusion, I have argued that the particular surface-state spectrum that is formed in smooth interfaces between a trivial and a topological insulator is a promising path towards the LL laser. In addition to the chiral surface state, which may be described in terms of a massless Dirac fermion, VP states are formed if the gap parameter varies over a width ℓ that must be larger than the intrinsic length scale $\lambda_C = \hbar v / \Delta$, in terms of the bulk gap Δ . These surface bands have the form of a massive 2D Dirac fermion, and each of the bands gives rise to LLs if a magnetic field is applied perpendicular to the interface. One is thus confronted with families of LLs the energy of which can to great extent be controlled, by the magnetic field for the LL separation and by the interface width for the energy separation between the VP bands. While the latter is given by the sample growth, it can still be varied *in situ* with the help of an inplane magnetic field that effectively reduces the interface width and thus increases the gap between the VP bands. The magnetic field does not only allow one to change the cyclotron frequency, at which light is emitted in certain setups, but

also to bring LLs associated with different VP bands into close energetic vicinity. When the gap between the VP bands is on the same order of magnitude as the typical LL separation – this situation can be easily achieved experimentally, *e.g.* in $\text{Pb}(1-x)\text{Sn}_x\text{Se}$ crystals – the LL spectra are neither equidistant nor follow a square-root law so that both Auger and reabsorption processes are maximally suppressed.

Another highly unusual and, for devices, potentially extremely fertile aspect of light emission in VP LLs is the direction of propagation of the absorbed and emitted photons. Indeed, photons with a wave vector perpendicular to the interface (Faraday geometry) are absorbed and emitted in transitions involving adjacent LL indices n and $n \pm 1$ but the same VP band index m , regardless of whether the LLs are formed in the positive- or negative energy branch of the VP bands. On the other hand, photons propagate inside the interface (Voigt geometry) for transitions $(m, n) \rightarrow (m \pm 1, n)$. This would allow for a smart design of the Fabry-Pérot cavities such that the extension in the z - and x/y -directions match the photon wavelength of the respective transitions, especially if pumping and emission are associated with the two different geometries (Faraday and Voigt). Finally, I have argued that the often detrimental Auger processes may be less efficient in the proposed setup so that they do not hinder the population inversion required for a LL laser, in contrast to most proposals for LL lasers.

ACKNOWLEDGMENTS

I would like to thank Gauthier Krizman, Louis-Anne de Vaultier, and Milan Orlita for fruitful discussions.

-
- [1] A. S. Tager and A. D. Gladun, *Sov. Phys. JETP* **8**, 560 (1959).
 - [2] P. A. Wolff, *Physics Physique Fizika* **1**, 147 (1964).
 - [3] H. Aoki, *Applied Physics Letters* **48**, 559 (1986).
 - [4] T. Morimoto, Y. Hatsugai, and H. Aoki, *Phys. Rev. B* **78**, 073406 (2008).
 - [5] E. Gornik, G. Strasser, and K. Unterrainer, *Nature Photonics* **15**, 875 (2021).
 - [6] M. Potemski, R. Stepniewski, J. C. Maan, G. Martinez, P. Wyder, and B. Etienne, *Phys. Rev. Lett.* **66**, 2239 (1991).
 - [7] D. B. But, M. Mittendorff, C. Consejo, F. Teppe, N. N. Mikhailov, S. A. Dvoretiskii, C. Faugeras, S. Winnerl, M. Helm, W. Knap, M. Potemski, and M. Orlita, *Nature Photonics* **13**, 783 (2019).
 - [8] B. Lax, *Cyclotron resonance and impurity levels in semiconductors. In Townes, C.H. (ed.) Proceedings of the International Symposium of Quantum Electronics* (Columbia University Press, New York, 1960).
 - [9] S. Gebert, C. Consejo, S. S. Krishtopenko, S. Ruffenach, M. Szola, J. Torres, C. Bray, B. Jouault, M. Orlita, X. Baudry, P. Ballet, S. V. Morozov, V. I. Gavrilenko, N. N. Mikhailov, S. A. Dvoretiskii, and F. Teppe, *Nature Photonics* **17**, 244 (2023).
 - [10] F. Wendler and E. Malic, *Scientific Reports* **5**, 12646 (2015).
 - [11] P. Plochocka, P. Kossacki, A. Golnik, T. Kazimierczuk, C. Berger, W. A. de Heer, and M. Potemski, *Phys. Rev. B* **80**, 245415 (2009).
 - [12] M. O. Goerbig, *Rev. Mod. Phys.* **83**, 1193 (2011).
 - [13] T. Kazimierczuk, A. Bogucki, T. Smoleński, M. Goryca, C. Faugeras, P. Machnikowski, M. Potemski, and P. Kossacki, *Phys. Rev. B* **100**, 075401 (2019).
 - [14] B. Volkov and O. Pankratov, *JETP Lett* **42**, 178 (1985).
 - [15] O. Pankratov, S. Pakhomov, and B. Volkov, *Solid state communications* **61**, 93 (1987).
 - [16] S. Tchoumakov, V. Jouffrey, A. Inhofer, E. Bocquillon, B. Plaçais, D. Carpentier, and M. O. Goerbig, *Phys. Rev. B* **96**, 201302 (2017).
 - [17] A. Inhofer, S. Tchoumakov, B. A. Assaf, G. Fève, J. M. Berroir, V. Jouffrey, D. Carpentier, M. O. Goerbig, B. Plaçais, K. Bendias, D. M. Mahler, E. Bocquillon, R. Schlereth, C. Brüne, H. Buhmann, and L. W. Molenkamp, *Phys. Rev. B* **96**, 195104 (2017).

- [18] D. M. Mahler, J.-B. Mayer, P. Leubner, L. Lunczer, D. Di Sante, G. Sangiovanni, R. Thomale, E. M. Hankiewicz, H. Buhmann, C. Gould, and L. W. Molenkamp, *Phys. Rev. X* **9**, 031034 (2019).
- [19] X. Lu and M. O. Goerbig, *Phys. Rev. B* **102**, 155311 (2020).
- [20] T. L. van den Berg, M. R. Calvo, and D. Bercioux, *Phys. Rev. Res.* **2**, 013171 (2020).
- [21] S. Tchoumakov, M. Civelli, and M. O. Goerbig, *Phys. Rev. B* **95**, 125306 (2017).
- [22] D. K. Mukherjee, D. Carpentier, and M. O. Goerbig, *Physical Review B* **100**, 195412 (2019).
- [23] T. L. van den Berg, A. De Martino, M. R. Calvo, and D. Bercioux, *Phys. Rev. Research* **2**, 023373 (2020).
- [24] D. J. Alspaugh, D. E. Sheehy, M. O. Goerbig, and P. Simon, *Phys. Rev. Research* **2**, 023146 (2020).
- [25] J. Bermejo-Ortiz, G. Krizman, R. Jakiela, Z. Khosravizadeh, M. Hajlaoui, G. Bauer, G. Springholz, L.-A. de Vaulchier, and Y. Guldner, *Phys. Rev. B* **107**, 075129 (2023).
- [26] G. Martinez, *Phys. Rev. B* **8**, 4686 (1973).
- [27] B. M. Wojek, P. Dziawa, B. J. Kowalski, A. Szczerbakow, A. M. Black-Schaffer, M. H. Berntsen, T. Balasubramanian, T. Story, and O. Tjernberg, *Phys. Rev. B* **90**, 161202 (2014).
- [28] G. Krizman, B. A. Assaf, T. Phuphachong, G. Bauer, G. Springholz, L. A. de Vaulchier, and Y. Guldner, *Phys. Rev. B* **98**, 245202 (2018).
- [29] X. Lu and M. O. Goerbig, *EPL (Europhysics Letters)* **126**, 67004 (2019).
- [30] Y. Wang, M. Tokman, and A. Belyanin, *Phys. Rev. A* **91**, 033821 (2015).